Supporting Information to:

Arsenic Species formed from Arsenopyrite Weathering along a Contamination Gradient in Circumneutral River Floodplain Soils

Petar N. Mandaliev,[†,§] Christian Mikutta,[†] Kurt Barmettler,[†] Tsvetan Kotsev,[‡]
and Ruben Kretzschmar[*,†]

[†]*Soil Chemistry Group, Institute of Biogeochemistry and Pollutant Dynamics, ETH Zurich, CHN, 8092 Zurich, Switzerland*

[‡]*Department of Geography, National Institute of Geophysics, Geodesy and Geography, Bulgarian Academy of Sciences, 1113 Sofia, Bulgaria*

(14 pages, 8 figures, 6 tables)

[§] Present address: Swiss Federal Office for the Environment, 3003 Bern

*Corresponding author e-mail: kretzschmar@env.ethz.ch;
 Phone: +41-44-6328758; Fax: +41-44-6331118

1. Study area

Ogosta River is one of the largest draining systems in North-West Bulgaria and its catchment involves more than 40 feeders. The river is 141 km long and covers an area of approximately 3110 km^2. The average altitude is 395 m, the mean river slope is 11.4‰, and the afforestation is ~37%.[1] The Ogosta River basin is strongly contaminated with As and other heavy metals (e.g., Pb, Cu, Zn, Cd) as result of intensive mining operations upstream.[2] The largest ore bodies in the mining area are Fe, Au, Ag-Pb, and fluorite-barite-calcite deposits, which are the products of Paleozoic and Alpine metallogenesis hosted in low-grade metamorphic rocks (marble and schist).[1] Between 1951 and 1999, ferrous-titanium, ferrous-manganese, and Pb/Zn-Au ores were intensively mined and processed in the mining area.[3] A large tailings dam failure in 1964 and the use of river water for irrigation of agricultural land additionally contributed to a significant dispersal of mining waste in the floodplain. Prior to the reconstruction of several tailing ponds, wastewater originating from several ore-dressing plants was discharged mostly into the river channel until 1979. Particularly the association of As with Fe minerals in the mining waste, notably pyrite (FeS$_2$) and arsenopyrite (FeAsS), led to high As concentrations in the floodplain soils.
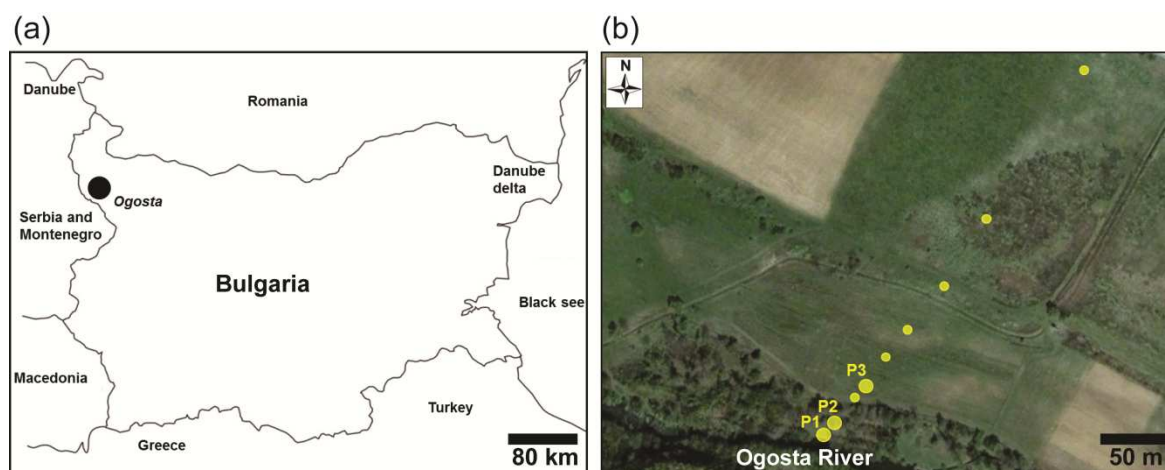

Figure S1. Location of (a) the Ogosta River floodplain in NW-Bulgaria, and (b) sampling points along the studied transect with soil profiles P1-3.

2. Soil characterization

P1 (1 m)   P2 (7 m)   P3 (49 m)

Figure S2. Photographs of soil profiles P1-3, which are located 1, 7, and 49 m from the river front, respectively (see Figure S1b).

Table S1. Physical and chemical characteristics of the bulk soil samples <2 mm.

Depth (cm)	pH (CaCl$_2$)	TIC[a]	TOC[b]	As	Fe	S	Mn	Ca	Al	As$_{asc}$[c]	Fe$_{asc}$[c]	As$_{asc}$/Fe$_{asc}$
		(%)					(g/kg)			(g/kg)		(mol/mol)
Profile 1												
0-5	6.7	0.1	8.5	7.1	73.8	2.1	7.1	37.0	36.4	4.1	12.8	0.23
8-10	5.8	1.1	0.6	40.3	164.6	4.6	15.3	18.3	25.4	-	-	-
10-20	6.6	1.4	0.5	32.4	145.8	29.9	14.0	51.6	20.3	18.2	40.2	0.34
20-30	6.9	2.3	0.2	20.3	124.4	24.6	14.1	97.8	18.5	11.8	32.5	0.27
30-40	6.8	1.8	0.1	28.1	187.5	31.5	24.6	73.4	16.1	7.5	30.5	0.18
40-50	6.9	2.0	0.1	30.3	187.5	27.6	21.8	83.2	17.1	5.4	29.5	0.14
50-60	7.0	3.8	0.3	9.3	120.0	0.78	21.5	105.0	24.8	7.1	26.8	0.20
60-70	6.7	3.8	0.2	8.6	120.1	0.73	19.7	103.3	24.6	7.1	29.9	0.18
70-80	6.9	3.5	0.3	10.1	131.5	3.4	18.7	94.8	24.8	5.5	24.6	0.17
80-90	6.2	1.9	0.5	25.7	171.5	2.3	23.0	18.5	20.6	16.9	40.5	0.31
90-100	5.7	1.7	0.6	38.8	195.2	5.8	27.6	11.8	24.8	15.3	33.5	0.34
Profile 2												
0-10	6.7	1.3	4.3	12.2	102.3	2.8	9.4	37.4	41.1	6.5	19.9	0.24
10-20	6.9	1.6	0.6	9.2	117.3	1.3	16.7	46.1	36.4	6.2	22.6	0.20
20-30	6.6	2.2	0.3	19.3	165.8	11.9	24.7	59.6	23.8	10.9	32.9	0.25
30-40	6.8	2.4	0.5	14.1	143.6	31.4	19.3	92.6	19.6	8.0	23.3	0.26
40-50	6.9	1.9	1.1	9.6	138.1	29.0	21.2	102.7	18.5	5.5	23.5	0.17
50-60	6.9	2.2	0.9	15.2	155.6	37.8	22.7	94.2	15.6	7.1	24.7	0.21
60-70	7.0	2.8	0.4	9.9	139.9	23.3	22.0	91.7	13.4	5.3	21.6	0.17
70-80	6.9	1.1	2.5	11.3	151.3	24.4	22.9	95.7	12.7	3.9	20.1	0.14
80-90	6.9	2.5	2.1	9.2	131.8	9.4	20.9	117.1	16.0	6.5	21.9	0.22
90-100	7.0	3.9	0.6	6.4	162.2	10.6	24.2	94.3	14.4	2.9	17.5	0.12
100-110	7.0	4.1	1.1	6.8	157.6	5.9	27.7	90.4	14.1	2.7	15.2	0.13
110-120	7.0	3.6	0.7	3.9	170.2	1.9	41.2	46.1	17.4	1.5	15.6	0.07
Profile 3												
0-10	7.0	0.4	1.4	0.9	57.7	0.5	6.4	21.8	53.5	0.6	7.5	0.06
10-20	7.0	0.4	1.2	0.9	57.8	0.4	6.6	22.6	52.3	0.5	5.9	0.06
20-30	7.1	0.6	0.9	0.7	61.7	0.3	7.9	24.9	52.3	0.4	8.9	0.03
30-40	7.1	0.8	0.9	0.9	66.0	0.5	8.4	30.0	52.8	0.5	8.9	0.04
40-50	7.0	0.4	0.8	0.3	53.9	0.2	5.6	16.7	56.3	0.2	5.7	0.02
50-60	6.7	0.1	0.4	0.04	39.4	0.1	1.3	7.8	60.1	<0.1	1.8	<0.01
60-70	6.6	0.01	0.7	0.08	43.2	0.2	2.0	7.1	65.8	<0.1	2.7	<0.01
70-80	6.8	0.01	0.3	0.07	45.6	0.1	1.7	9.7	59.4	<0.1	2.1	<0.01
Pearson correlation coefficients												
As				1	0.75***	0.45*	0.41*	0.08	-0.56**			
Fe					1	0.55**	0.89***	0.51**	-0.91***			
S						1	0.37*	0.58**	-0.63***			
Mn							1	0.56**	-0.86***			
Ca								1	-0.77***			
Al									1			

[a]Total inorganic carbon. [b]Total organic carbon. [c]Ascorbate-extractable As and Fe.

*Significance level *P* <0.05, **significance level *P* <0.01, ***significance level *P* <0.001.

Table S2. Physical and chemical characteristics of the 2-50 μm and <2 μm particle size fractions.

Depth (cm)	Fraction 2-50 μm	Fraction <2 μm	TC[a] 2-50 μm	TC[a] <2 μm	As 2-50 μm	As <2 μm	Fe 2-50 μm	Fe <2 μm	Mn 2-50 μm	Mn <2 μm	S 2-50 μm	S <2 μm	As$_{asc}$[b] 2-50 μm	As$_{asc}$[b] <2 μm	Fe$_{asc}$[b] 2-50 μm	Fe$_{asc}$[b] <2 μm	As$_{asc}$/Fe$_{asc}$ 2-50 μm	As$_{asc}$/Fe$_{asc}$ <2 μm
	(%)						(g/kg)										(mol/mol)	
Profile 1																		
0-5	10.5	-	5.1	-	15.4	-	91.1	-	4.7	-	2.1	-	-	-	-	-	-	-
8-10	17.2	3.4	0.9	2.1	86.4	89.7	266.2	236.1	8.5	11.1	4.0	0.4	26.2	62.2	40.4	115.8	0.48	0.39
10-20	18.8	3.0	0.7	1.9	100.8	53.2	266.3	154.2	6.2	10.2	16.9	4.3	48.1	-	74.7	-	0.48	-
20-30	15.4	-	1.1	-	65.6	-	251.4	-	11.9	-	16.2	-	35.1	-	66.9	-	0.39	-
30-40	11.2	3.5	1.2	1.6	72.5	50.2	298.2	255.1	17.0	25.4	12.7	2.9	29.0	25.9	60.2	99.8	0.36	0.19
40-50	8.5	-	0.4	-	62.8	-	318.7	-	16.8	-	13.6	-	8.1	-	25.8	-	0.23	-
50-60	39.8	4.8	0.4	2.5	13.8	51.6	150.3	217.3	23.1	15.5	0.9	1.6	7.1	34.6	22.4	94.5	0.23	0.22
60-70	31.1	-	0.2	-	14.9	-	167.1	-	22.4	-	0.9	-	9.8	-	39.2	-	0.19	-
70-80	43.6	3.9	0.2	2.8	12.8	43.4	152.2	221.2	19.1	18.4	4.7	0.5	5.9	28.7	24.1	88.5	0.18	0.24
80-90	13.3	-	0.2	-	81.4	-	271.6	-	8.6	-	2.9	-	52.5	-	86.4	-	0.45	-
90-100	5.7	3.1	0.3	2.8	102.8	214.0	337.3	418.4	17.3	31.3	2.5	0.6	46.7	66.9	83.7	129.2	0.41	0.35
Profile 2																		
0-10	14.1	2.1	2.6	2.4	35.6	23.4	142.4	149.3	6.3	16.7	3.4	0.2	20.8	19.2	47.1	54.7	0.33	0.26
10-20	7.6	-	0.3	-	72.1	-	284.3	-	7.6	-	4.6	-	39.2	-	65.1	-	0.45	-
20-30	10.5	-	0.3	-	89.6	-	325.7	-	8.7	-	12.5	-	42.1	-	70.1	-	0.45	-
30-40	11.2	1.8	0.1	2.2	58.9	41.4	297.1	177.2	10.9	21.6	14.7	1.5	30.6	17.6	67.3	34.2	0.34	0.38
40-50	7.6	-	1.4	-	52.8	-	341.9	-	14.1	-	14.1	-	-	-	-	-	-	-
50-60	10.7	2.2	0.4	2.5	60.2	39.7	292.8	207.4	14.6	25.2	10.9	1.6	16.2	25.3	33.9	80.1	0.36	0.24
60-70	6.6	-	1.2	-	43.3	-	297.6	-	20.2	-	12.9	-	9.6	-	33.1	-	0.21	-
70-80	8.9	2.1	0.7	3.5	43.8	31.4	282.3	224.1	20.1	33.7	7.7	1.5	12.5	16.1	34.7	66.3	0.27	0.18
80-90	32.8	-	2.0	-	15.4	-	167.4	-	22.1	-	2.9	-	8.9	-	25.2	-	0.27	-
90-100	17.6	-	0.6	-	14.4	-	242.8	-	25.7	-	3.1	-	4.7	-	21.5	-	0.16	-
100-110	22.7	-	1.6	-	12.4	-	201.2	-	30.1	-	4.9	-	3.1	-	18.3	-	0.12	-
110-120	6.2	-	0.6	-	15.3	-	241.7	-	42.9	-	1.8	-	3.0	-	20.8	-	0.11	-
Profile 3																		
0-10	11.1	2.1	1.7	2.7	1.3	7.2	67.1	109.1	11.4	11.4	0.4	0.2	0.8	3.4	13.1	16.9	0.05	0.15
10-20	10.3	-	1.3	-	1.3	-	68.4	-	8.2	-	0.4	-	0.9	-	13.8	-	0.05	-
20-30	11.4	-	1.3	-	1.5	-	82.1	-	1.2	-	0.5	-	0.9	-	21.3	-	0.03	-
30-40	10.6	1.8	1.3	2.8	1.7	5.1	82.4	109.6	1.1	10.2	0.6	0.2	-	3.6	-	33.3	-	0.08
40-50	12.0	-	1.1	-	1.1	-	78.5	-	1.1	-	0.4	-	-	-	-	-	-	-
50-60	6.2	-	0.7	-	0.06	-	44.5	-	1.5	-	0.1	-	-	-	-	-	-	-
60-70	2.6	-	0.4	-	0.04	-	51.6	-	2.8	-	0.2	-	-	-	-	-	-	-
Pearson correlation coefficients																		
As							0.84***	0.92***	-0.04	0.42	0.66***	-0.02						
Fe							1	1	0.38*	0.67**	0.74***	-0.01						
Mn									1	1	0.07	0.07						
S											1	1						

[a]Total carbon. [b]Ascorbate-extractable As and Fe. *Significance level $P <0.05$, **significance level $P <0.01$, ***significance level $P <0.001$.
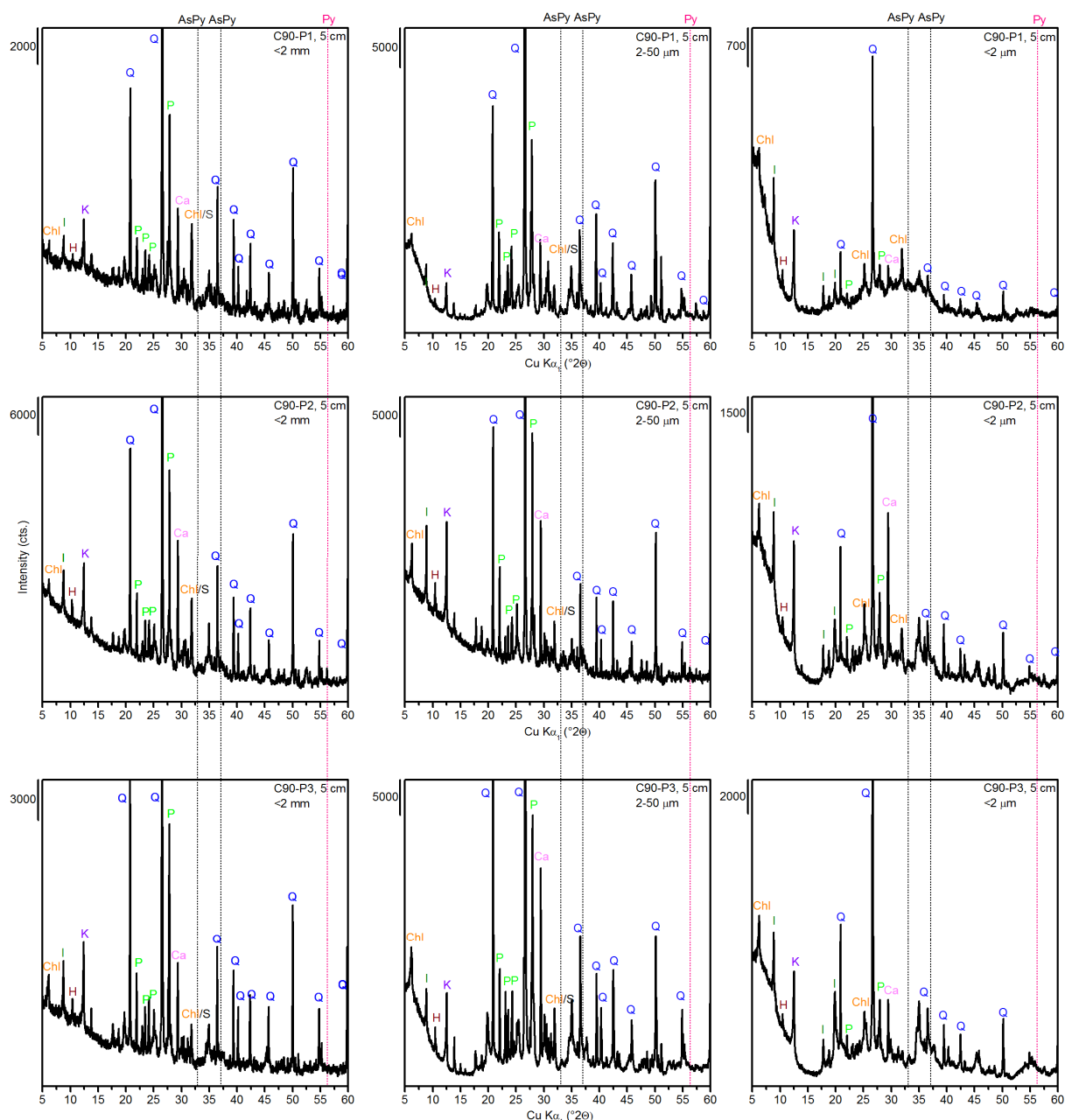
Figure S3. XRD patterns of the <2 mm, 2-50 µm, and <2 µm particle size fractions of selected top-soil samples from soil profiles P1-3. The main peaks are labeled as follows: Q, quartz; Ca, calcite; H, hornblende; K, kaolinite; I, illite; Chl, chlorite; S, siderite; P, plagioclase. Peak positions for pyrite and arsenopyrite are marked with dashed lines (AsPy and Py).

3. Arsenic reference compounds

Table S3. Arsenic reference compounds analyzed by XAS (Figure S4).

Compound	Chemical formula	Source/synthesis
Arsenopyrite	FeAsS	natural[a]
Loellingite	FeAs$_2$	natural[a]
Orpiment	As$_2$S$_3$	natural[a]
Realgar	α-As$_4$S$_4$	natural[a]
Pharmacolite	CaHAsO$_4$·2H$_2$O	natural[a]
Arseniosiderite	(Ca$_2$Fe$_3$O$_2$(AsO$_4$)$_3$·2H$_2$O)	natural[b]
Pharmacosiderite	(KFe$_4$(AsO$_4$)$_3$(OH)$_4$·6H$_2$O)	natural[a]
Scorodite	FeAsO$_4$·2H$_2$O	natural[a]
Amorphous ferric arsenate (AFA)	FeAsO$_4$·(2+n)H$_2$O	synthetic[c]
As(V)-Fh	As(V) sorbed to ferrihydrite (As/Fe ~0.05)	synthetic[d]
As(III)-Fh	As(III) sorbed to ferrihydrite (As/Fe ~0.05)	synthetic[d]

[a]Provided by the mineralogical collection of TU Bergakademie Freiberg (Germany). [b]Provided by the mineralogical collection of ETH Zurich (Switzerland). [c]Mikutta et al.[4]. [d]Langner et al.[5].
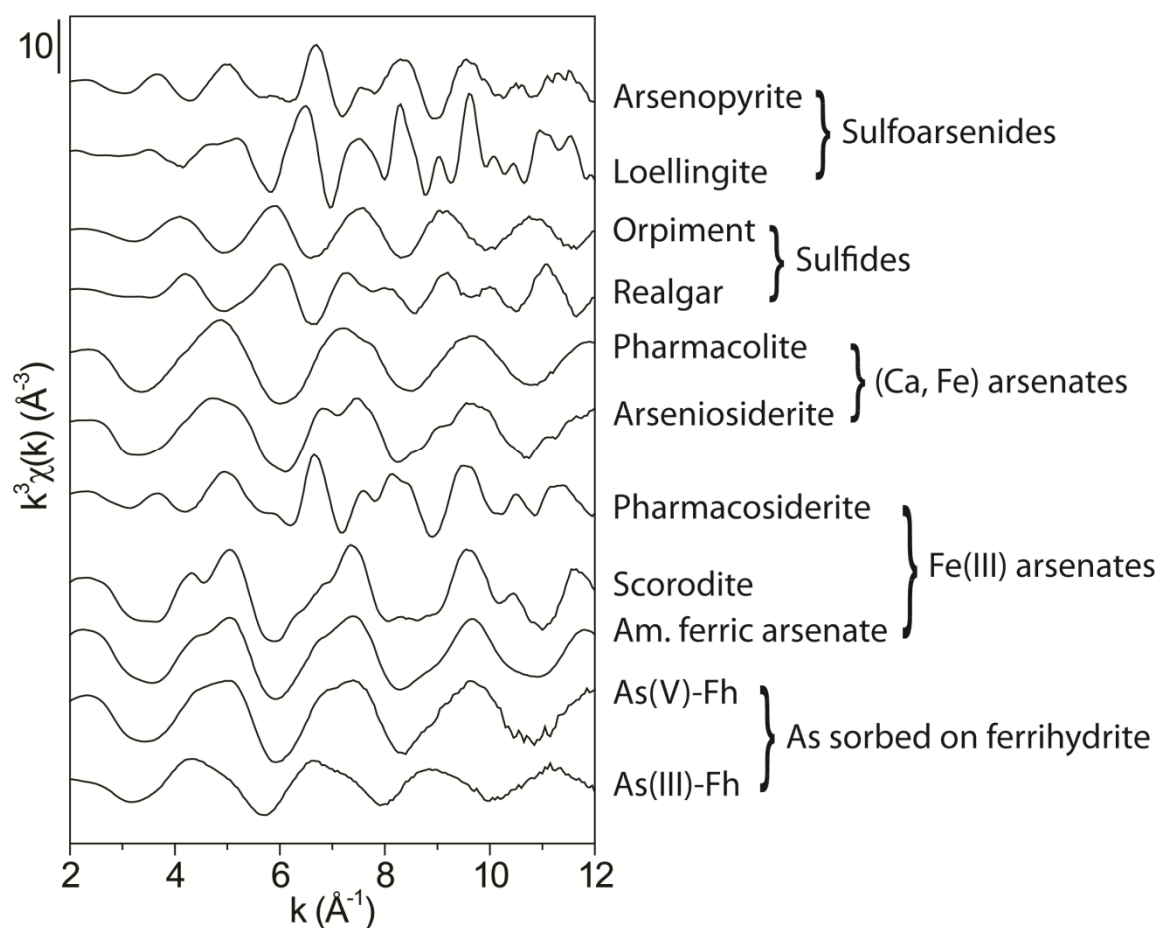
Figure S4. k^3-weighted As K-edge EXAFS spectra of As reference compounds.
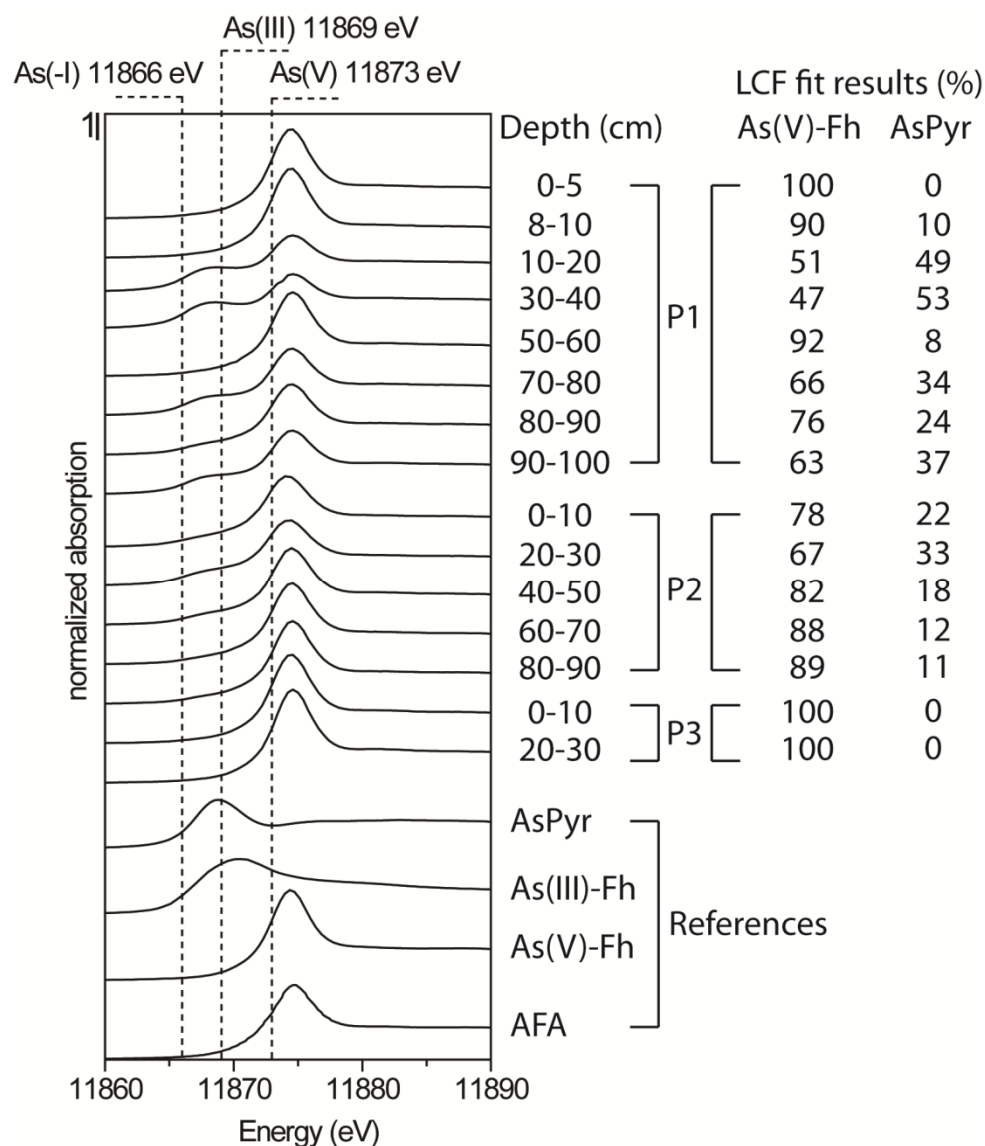
4. As XANES analysis

Figure S5. Normalized As *K*-edge XANES spectra for selected <2 mm soil samples and As reference compounds and linear combination fitting results using As(V)-sorbed ferrihydrite (As(V)-Fh) and arsenopyrite (AsPyr) as reference compounds in the final fits. As(III) was not detected in any of the samples. In the final fits, the sum of As in As(V)-Fh and AsPyr was constrained to 100%.

5. Iron reference compounds

Table S4. Iron reference compounds analyzed by XAS (Figure S6).

Compound	Chemical formula	Source/synthesis
Pyrite	FeS_2	natural[a]
Arsenopyrite	FeAsS	natural[b]
Chlorite (Ripidolite, Cca-2)	$(Ca_{0.55})(Mg_{4.44}Fe(III)_{3.47}Fe(II)_{3.02}Al_{0.60}Mn_{0.01}Ti_{0.06})(Si_{4.51}Al_{13.49})O_{20}(OH)_{16}$	natural[c]
Siderite	$FeCO_3$	natural[a]
Scorodite	$FeAsO_4 \cdot 2H_2O$	natural[b]
Amorphous ferric arsenate (AFA)	$FeAsO_4 \cdot (2+n)H_2O$	synthetic[d]
As-HFO-0.39	Fe(III)-As(V) coprecipitate (molar As/Fe ratio = 0.39)	synthetic[e]
Ferrihydrite	$Fe_{10}O_{14}(OH)_2Fe(OH)_3$	synthetic[f]
Goethite	α-FeOOH	synthetic[f]
Lepidocrocite	γ-FeOOH	synthetic[f]
Magnetite	Fe_3O_4	natural[a]

[a]Provided by the mineralogical collection of ETH Zurich (Switzerland). [b]Provided by the mineralogical collection of TU Bergakademie Freiberg (Germany). [c]Source Clays Repository (Origin: Flagstaff Hill, El Dorado County, CA, USA). [d]Mikutta et al.[4] [e]This study. [f]Langner et al.[5]
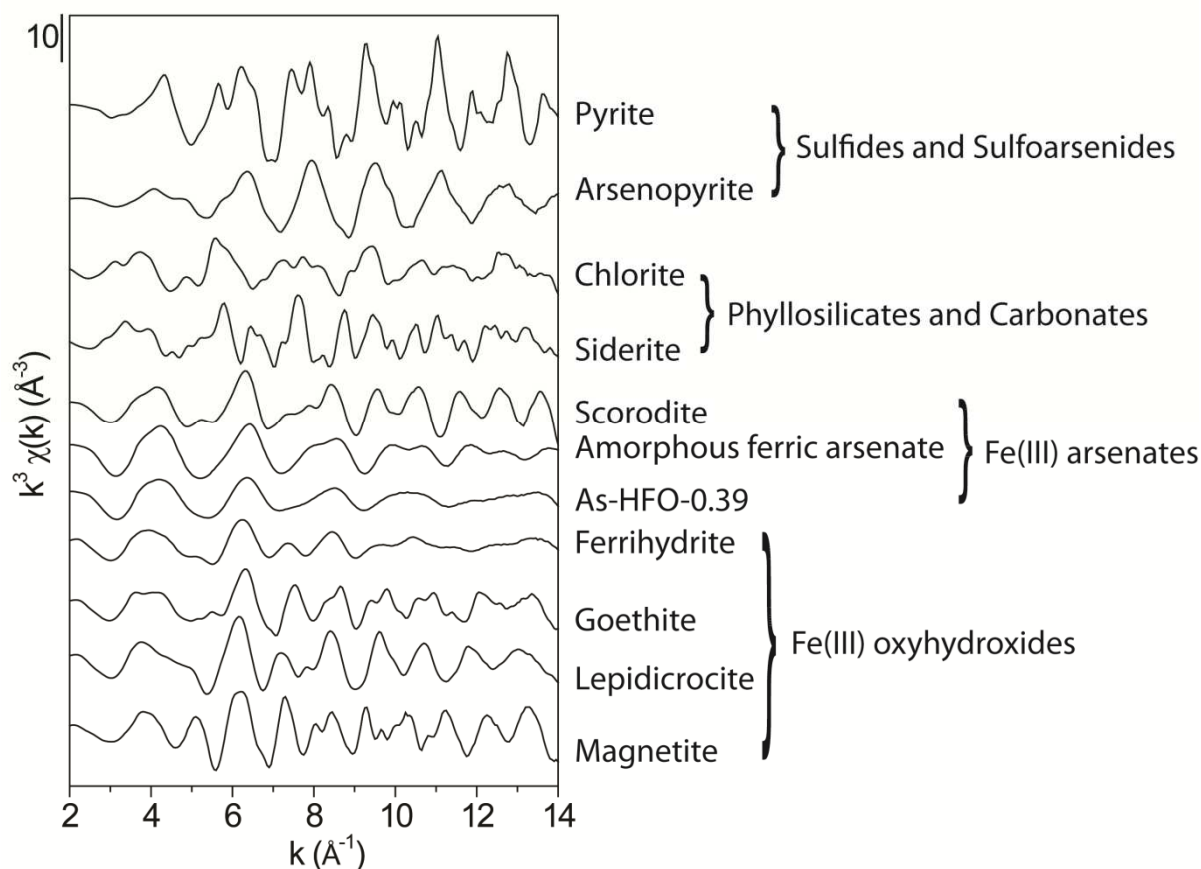

Figure S6. k^3-weighted Fe K-edge EXAFS spectra of Fe reference compounds. The As-HFO-0.39 reference sample is an As-rich hydrous ferric oxide with a molar As/Fe ratio of 0.39.
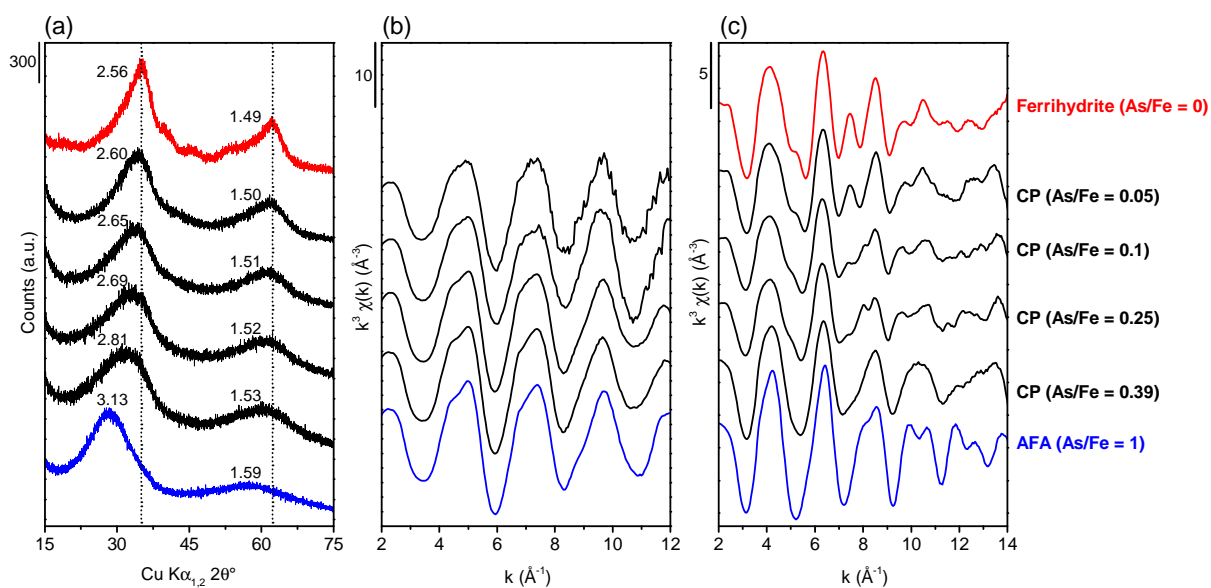
Figure S7. (a) X-ray diffraction patterns, (b) As *K*-edge EXAFS, and (c) Fe *K*-edge EXAFS spectra of pure ferrihydrite (no As EXAFS), a range of Fe(III)-As(V) coprecipitates (CP) with molar As/Fe ratios of 0.05-0.39, and amorphous ferric arsenate (AFA). Numbers in (a) refer to the approximate interplanar *d*-spacings of the peak maxima in Ångstrom. The CP (As/Fe = 0.39) sample corresponds to the As-HFO-0.39 reference used for linear combination fitting (LCF) of Fe EXAFS spectra.

6. XAS data reduction and analysis

XAS data reduction and linear combination fitting (LCF) were performed using Athena.[6] Principal component analysis (PCA) and target transformation (TT) testing were performed using SIXPack.[7] Absorption spectra were normalized using a linear function in the pre-edge region (-200 to -30 eV relative to the edge energy E_0) and a quadratic polynomial in the post-edge region (150 eV to 690 eV relative to E_0). The EXAFS spectra were extracted using the Autobk algorithm implemented in Athena (k-weight = 3). Linear combination fit analyses were carried out over the k-range 3.0-12.0 Å^{-1}. Starting from a single component fit ($n = 1$) yielding the lowest normalized sum of squared residual value, *NSSR*, the number of components was stepwise increased as long as the *NSSR* of the best $n+1$-component fit was at least 10% below the *NSSR* of the best n-component fit. The fitted fraction of each spectrum was constrained between 0 and 1, but the component sum was not forced to 100% in order to obtain component ratios.

Iron and As K-edge EXAFS spectra of the <2 mm, 2-50 μm, and <2 μm soil fractions were evaluated by PCA-TT in order to determine the number of statistically significant spectral components contributing to the EXAFS spectra.[8, 9] The PCA-TT analysis was carried out on k^3-weighted As and Fe K-edge EXAFS spectra over a k-range of 3.0-12.0 Å^{-1} using the same E_0 for all samples (11873 eV for As and 7128 eV for Fe). The PCA analysis revealed that 2-3 spectral components were needed to reproduce the set of soil As EXAFS spectra, whereas 3-4 spectral components were required to reproduce the set of soil Fe EXAFS spectra. The suitability of Fe and As reference spectra for LCF was further assessed by TT using the first 3-4 components calculated with PCA. This assessment is based on the classification of the As and Fe reference spectra using the empirical SPOIL value.[10, 11] Arsenic and Fe EXAFS references (Tables S3 and S4) were classified as excellent (SPOIL 0-1.5), good (SPOIL 1.5-3), fair (SPOIL 3-4.5), acceptable (SPOIL 4.5-6), and unacceptable (SPOIL >6).[11] For the As EXAFS references, TT analysis resulted in SPOIL values (<4.5) for the following As reference compounds: arsenopyrite, As(V)-ferrihydrite, AFA, As-HFO-0.39, and pharmacolite. For the Fe EXAFS references, TT analysis resulted in acceptable SPOIL values for arsenopyrite, ferrihydrite, AFA, As-HFO-0.39, chlorite, siderite, pyrite, goethite, and magnetite. Poor spectra reconstructions with higher SPOIL values (>4.5) were found for all other As and Fe reference spectra.

The Fe K-edge EXAFS of the As-HFO-0.39 sample was extracted using the Autobk algorithm implemented in Athena[12] (k-weight = 3). The frequency cut-off parameter, R_{bkg}, was set to 0.85 and E_0 was defined as the maximum of the first XANES derivative (7127.4 eV). The pre-edge region was fitted with a linear function and the post-edge region with a quadratic polynomial. The Fourier transform was calculated over k = 2.0-12.5 Å^{-1} using a Kaiser-Bessel apodization window with a sill width of 3 Å^{-1}. Shell fits were performed in R-space over $R + \Delta R$ = 1.0-4.0 Å in Artemis[12] (fit k-weight = 3). Theoretical phase-shift and amplitude functions were calculated with FEFF v.8.4 based on the structures of scorodite[13] and goethite.[14] The passive amplitude reduction factor, S_0^2, was set to 0.9, and the degeneracies and Debye-Waller parameters, σ^2, of octahedral multiple scattering paths were defined in terms of the Fe-O shell.[15]

7. LCF analysis

Table S5. Linear combination fitting (LCF) results of Fe EXAFS spectra of selected samples from soil profile P1, including either amorphous ferric arsenate (AFA) or As-HFO-0.39 (an Fe(III)-As(V) coprecipitate with a molar As/Fe ratio of 0.39) as possible Fe reference in the LCF (see box for further explanation).

Depth	Size fraction	AsPyr	Fh	AFA	As-HFO-0.39	Sid	Chl	Sum	$NSSR$[a]	As in AFA or As-HFO-0.39 (Fe EXAFS)	As in AsPyr (As EXAFS)	As in AFA or As-HFO-0.39 + AsPyr (Fe and As EXAFS)	As in AsPyr (Fe EXAFS)
(cm)			(%) (normalized to sum = 100)					(%)			(% of total As)		
0-10	<2 mm		56			19	25	92	8.4				
	<2 mm		41	15		18	26	86	6.2	280	19	299	
	<2 mm		37		20	19	24	94	7.1	109	19	128	
	2-50 µm	5	66			10	18	96	4.6				
	2-50 µm	6	50	16		10	19	91	2.1	131	35	167	43
	2-50 µm	5	41		25	11	18	97	2.1	79	35	79	39
	<2 µm		86				14	82	9.2				
	<2 µm		54	36			10	89	2.3	98		98	
	<2 µm		26		61		13	93	1.8	83		83	
30-40	<2 mm	6	58			12	24	93	7.7				
	<2 mm	6	45	13		12	24	89	6.1	124	50	174	53
	<2 mm	6	41		17	12	24	92	7.0	48	50	98	53
	2-50 µm	8	81				10	102	4.5				
	2-50 µm	9	62	18			11	100	2.5	101	22	123	49
	2-50 µm	7	45		36		11	104	2.4	81	22	103	38
	<2 µm		86				14	92	4.7				
	<2 µm		70	18			12	91	1.9	105	20	125	
	<2 µm		49		38		13	96	1.8	90	20	110	
70-80	<2 µm		77				23	101	6.2				
	<2 µm		59	15			26	88	3.7	138	8	146	
	<2 µm		50		26		24	99	4.6	71	8	79	
90-100	2-50 µm	3	78			5	12	83	5.4				
	2-50 µm	5	60	18		4	14	84	1.5	79	11	90	22
	2-50 µm	3	37		43	5	12	86	1.9	65	11	76	13
	<2 µm		86				14	89	10.9				
	<2 µm		54	36			10	86	2.3	79	5	84	
	<2 µm		26		61		13	97	1.8	49	5	54	

Explanation:

Each sample was fitted three times:
(i) without AFA and As-HFO-0.39
(ii) with AFA
(iii) with As-HFO-0.39
as possible Fe reference.

All fits included arsenopyrite (AsPyr), ferrihydrite (Fh), siderite (Sid), and chlorite (Chl) as Fe references.

From the fitted amounts of AFA or As-HFO-0.39 (Fe EXAFS), the theoretical amounts of As present in these phases were calculated (in % of total As) to test the plausibility of the Fe EXAFS fits.

To these values, the amounts of As in arsenopyrite determined by As EXAFS were added.

For comparison, the amounts of As in arsenopyrite from Fe EXAFS are provided in the last column (only for the fits with AFA or As-HFO-0.39).

[a]Normalized sum of the squared residuals (NSSR (%) = $100\Sigma(\text{data}_i - \text{fit}_i)^2/\Sigma(\text{data}_i)^2$).

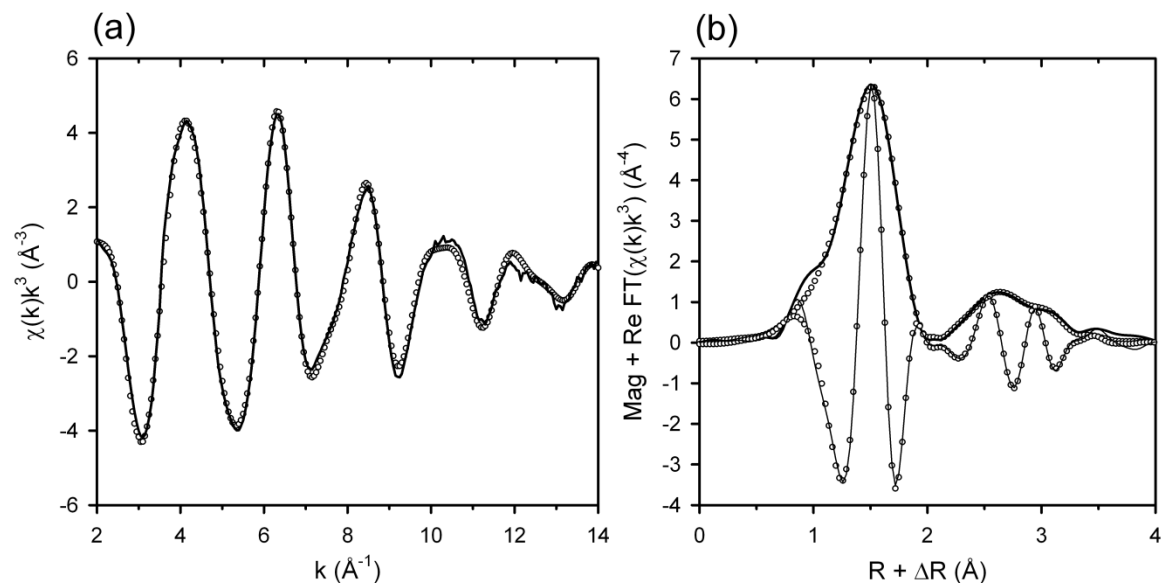# 8. Shell-fit analysis of reference sample As-HFO-0.39

Figure S8. (a) k^3-weighted Fe K-edge EXAFS of the Fe(III)-As(V) coprecipitate with a molar As/Fe ratio of 0.39 (As-HFO-0.39), as well as (b) magnitude and real part of the Fourier-transformed EXAFS. Experimental data and the fit are shown as solid and dotted line, respectively. Shell-fit parameters are summarized in Table S6.

Table S6. EXAFS parameters determined by shell fitting of the Fe K-edge EXAFS spectrum of the As-HFO-0.39 sample.[a]

Path	CN[b]	R (Å)[c]	σ^2 (Å^2)[d]	ΔE (eV)[e]	R-Factor[f]	redχ^{2}[g]
Fe-O	4.4(2)	1.98(0)	0.008(0)	4.2(5)	0.003	212
Fe-Fe	2.3(8)	3.08(1)	0.019(5)			
Fe-As	0.39	3.32(2)	0.006(2)			
Fe-O-O[h]	17.8	3.40(7)	0.015			
Fe-O-Fe-O[i]	4.4	3.90(3)	0.015			

[a]Parameter uncertainties are given in parentheses for the last significant figure. Parameters without error assignment were fixed or constrained in the fit. [b]Coordination number (path degeneracy). [c]Mean half path length. [d]Debye-Waller parameter. [e]Energy-shift parameter. [f]R-factor = $\sum_i(data_i-fit_i)^2/\sum_i data$. [g]Reduced χ^2 = $n_{idp}/n_{pts}\sum_i((data_i-fit_i)/\varepsilon_i)^2(n_{idp}-n_{var})^{-1}$, where n_{idp}, n_{pts}, and n_{var} are, respectively, the number of independent points in the model fit, the total number of data points, the number of fit variables, and ε_i is the uncertainty of the ith data point (n_{idp}/n_{var} = 20/11). [h]CN = 4CN(Fe-O) and σ^2 = 2σ^2(Fe-O). [i]CN = CN(Fe-O) and σ^2 = 2σ^2(Fe-O).

9. References

1. Angelova, D., Integral environmental assessment of Ogosta River basin (northwestern Bulgaria). In *BALWOIS 2008*, Ohrid, Republic of Macedonia, 2008; p 15.
2. Mladenova, V.; Kotsev, T.; Ivanova, I.; Cholakova, Z.; Dimitrova, D.; Schmitt, R.-T. In *Mineralogy of the heavy metal and metalloid pollution of the Ogosta river floodplains, NW Bulgaria*, Proceedings of Geosciences 2008, Sofia, Bulgaria, 2008; pp 121-122.
3. Bird, G.; Brewer, P. A.; Macklin, M. G., Management of the Danube drainage basin: Implications of contaminant-metal dispersal for the implementation of the EU water framework directive. *Intl. J. River Basin Management* **2010,** *8*, 63 - 78.
4. Mikutta, C.; Mandaliev, P. N.; Kretzschmar, R., New clues to the local atomic structure of short-range ordered ferric arsenate from extended X-ray absorption fine structure spectroscopy. *Environ. Sci. Technol.* **2013,** *47*, 3122-3131.
5. Langner, P.; Mikutta, C.; Kretzschmar, R., Arsenic sequestration by organic sulphur in peat. *Nature Geosci.* **2012,** *5*, 66-73.
6. Ravel, B.; Newville, M., ATHENA and ARTEMIS: Interactive graphical data analysis using IFEFFIT. *Phys. Scripta* **2005,** *T115*, 1007-1010.
7. Webb, S. M., SIXPack: A graphical user interface for XAS analysis using IFEFFIT. *Phys. Scripta* **2005,** *T115*, 1011-1014.
8. Jacquat, O.; Voegelin, A.; Villard, A.; Marcus, M. A.; Kretzschmar, R., Formation of Zn-rich phyllosilicate, Zn-layered double hydroxide and hydrozincite in contaminated calcareous soils. *Geochim. Cosmochim. Acta* **2008,** *72*, 5037-5054.
9. Voegelin, A.; Scheinost, A. C.; Buhlmann, K.; Barmettler, K.; Kretzschmar, R., Slow formation and dissolution of Zn precipitates in soil: A combined column-transport and XAFS study. *Environ. Sci. Technol.* **2002,** *36*, 3749-3754.
10. Beauchemin, S.; Hesterberg, D.; Beauchemin, M., Principal component analysis approach for modeling sulfur K-XANES spectra of humic acids. *Soil Sci. Soc. Am. J.* **2002,** *66*, 83-91.
11. Malinowski, E. R., Theory of error for target factor analysis with applications to mass spectrometry and nuclear magnetic resonance spectrometry. *Anal. Chim. Acta.* **1978,** *103*, 339-354.
12. Ravel, B.; Newville, M., ATHENA, ARTEMIS, HEPHAESTUS: data analysis for X-ray absorption spectroscopy using IFEFFIT. *J. Synchrotron Radiat.* **2005,** *12*, 537-541.
13. Kitahama, K.; Kiriyama, R.; Baba, Y., Refinement of the crystal structure of scorodite. *Acta Cryst. B* **1975,** *31*, 322-324.
14. Kaur, N.; Singh, B.; Gräfe, M., Substitution of multimetals in goethite. *Geochim. Cosmochim. Acta* **2006,** *70*, A308.
15. Voegelin, A.; Kaegi, R.; Frommer, J.; Vantelon, D.; Hug, S. J., Effect of phosphate, silicate, and Ca on Fe(III)-precipitates formed in aerated Fe(II)- and As(III)-containing water studied by X-ray absorption spectroscopy. *Geochim. Cosmochim. Acta* **2010,** *74*, 164-186.